

See discussions, stats, and author profiles for this publication at: <https://www.researchgate.net/publication/231661289>

Synthesis and Structural Characterization of Microporous Yttrium and Calcium Silicates

ARTICLE in THE JOURNAL OF PHYSICAL CHEMISTRY B · JUNE 1998

Impact Factor: 3.3 · DOI: 10.1021/jp9803337

CITATIONS

28

READS

34

6 AUTHORS, INCLUDING:



Joao Rocha

University of Aveiro

455 PUBLICATIONS 9,801 CITATIONS

SEE PROFILE



Paula Ferreira

University of Aveiro

108 PUBLICATIONS 1,410 CITATIONS

SEE PROFILE



Zhi Lin

University of Aveiro

130 PUBLICATIONS 1,645 CITATIONS

SEE PROFILE



Artur Ferreira

University of Aveiro

72 PUBLICATIONS 1,739 CITATIONS

SEE PROFILE

Synthesis and Structural Characterization of Microporous Yttrium and Calcium Silicates

João Rocha,* Paula Ferreira, Zhi Lin, Paula Brandão, A. Ferreira, and J. D. Pedrosa de Jesus

Department of Chemistry, University of Aveiro, 3810 Aveiro, Portugal

Received: November 25, 1997; In Final Form: April 6, 1998

The synthesis and structural characterization of AV-1 (Aveiro microporous solid no. 1), the first synthetic microporous yttrium silicate containing stoichiometric amounts of framework sodium (and yttrium) cations, are reported. AV-1, $\text{Na}_4\text{K}_2\text{Y}_2\text{Si}_{16}\text{O}_{38}\cdot 10\text{H}_2\text{O}$, possesses the structure of the rare mineral montregianite. The synthesis and structural characterization of AV-2, an alkali calcium silicate hydrate (ideal composition $\text{HKCa}_2\text{Si}_8\text{O}_{19}\cdot 6\text{H}_2\text{O}$) analogue of the rare mineral rhodesite, are also reported. The structures of AV-1 and AV-2 are characterized by the same type of double silicate layers, but important differences exist with respect to the constitution of the octahedral layers and channel species. AV materials have been characterized by a range of techniques, viz., scanning electron microscopy (SEM), powder X-ray diffraction (XRD), ^{29}Si and ^{23}Na single- and triple-quantum (3Q) magic-angle spinning (MAS) NMR spectroscopy, Fourier transform spectroscopy (FTIR), and thermogravimetric analysis (TGA).

Introduction

Zeolites are well-known crystalline hydrated aluminosilicates with open three-dimensional framework structures built of $[\text{SiO}_4]^{4-}$ and $[\text{AlO}_4]^{5-}$ tetrahedra. These materials are of considerable technological importance as shape-selective catalysts, ion-exchange solids, and molecular sieves. Many other materials with zeolite-type structures, particularly porous aluminophosphates and derivatives, are known, all of which contain tetrahedrally coordinated metal atoms.¹ Recently, much research has been carried out aimed at preparing inorganic microporous framework solids containing atoms with different coordination geometries. One such family of materials is of considerable interest, microporous titanosilicates (known as ETS materials) and derivatives containing Ti^{4+} usually in octahedral coordination.^{2–4} We have been interested in the synthesis of microporous framework silicates of several elements of the periodic table.^{5–7}

Recently, we have briefly reported the synthesis and characterization of AV-1, a sodium yttrium silicate possessing the structure of the mineral montregianite.⁸ We now wish to expound on these studies and to describe the synthesis and characterization of AV-2, the synthetic analogue of the mineral rhodesite, a microporous calcium silicate with a structure closely related to the structure of montregianite and AV-1. Montregianite (also known as UK-6) is a very rare hydrous sodium potassium yttrium silicate ($\text{Na}_4\text{K}_2\text{Y}_2\text{Si}_{16}\text{O}_{38}\cdot 10\text{H}_2\text{O}$) from Mont St. Hilaire, Québec, Canada, where it occurs in miarolitic cavities and thermally metamorphosed inclusions and rheomorphic breccias in nepheline syenite.^{9,10} The structure of montregianite (and AV-1) is very unusual because the sodium (and yttrium) cations are an integral part of the framework. In sharp contrast, in zeolites and zeolite-type materials the charge-balancing sodium cations usually reside within the channels and, thus, are not part of the framework. Rhodesite was described first in 1957 as an alkali calcium silicate hydrate from the Bultfontein diamond mine in Kimberley, South Africa.¹¹ Hesse et al. solved the structure of rhodesite specimens from Zeilberg (Germany), Trinity County (California, USA), and San Venanzo (Italy) and defined the ideal composition of the mineral as

$\text{HKCa}_2\text{Si}_8\text{O}_{19}\cdot 6\text{H}_2\text{O}$.^{12,13} Although montregianite and rhodesite are characterized by the same type of double silicate sheets, important differences exist with respect to the constitution of the octahedral layers and channel species.

Experimental Section

Synthesis. The syntheses of AV materials were carried out in Teflon-lined autoclaves, under static hydrothermal conditions, in ovens preheated at 230 °C. In all syntheses, the autoclaves were removed and quenched in cold water after the appropriate time. The crystals were filtered, washed at room temperature with distilled water, and dried at 100 °C.

Typical AV-1 Synthesis. An alkaline solution was made by mixing 5.07 g of sodium silicate solution (27% m/m SiO_2 , 8% m/m Na_2O , Merck), 18.3 g of H_2O , 0.20 g of KOH (Carlo Erba), 0.29 g of NaOH (Merck), and 0.22 g of NaCl (Aldrich). A 1.73 g sample of $\text{Y}_2(\text{SO}_4)_3\cdot 8\text{H}_2\text{O}$ (Aldrich) was added to this solution and stirred thoroughly. The gel, with a composition 0.53 Na_2O :0.078 K_2O :1.0 SiO_2 :0.12 Y_2O_3 :44 H_2O , was autoclaved for 6 days.

Typical AV-2 Synthesis. An alkaline solution was made by mixing 5.07 g of sodium silicate solution (27% m/m SiO_2 , 8% m/m Na_2O , Merck), 15.2 g of H_2O , 0.20 g of KOH (Carlo Erba), 0.28 g of NaOH (Merck) and 0.22 g of NaCl (Aldrich). A 0.70 g sample of $\text{Ca}(\text{NO}_3)_2\cdot 4\text{H}_2\text{O}$ (Panreac) was added to this solution and stirred thoroughly. The gel, with a composition 0.52 Na_2O :0.080 K_2O :1.0 SiO_2 :0.13 CaO :37 H_2O , was autoclaved for 6 days.

Techniques. Powder XRD data were collected on a Rigaku diffractometer using $\text{Cu K}\alpha$ radiation filtered by Ni. SEM images were recorded on a Hitachi S-4100 microscope. ^{29}Si and ^{23}Na MAS NMR spectra were recorded at 79.49 and 105.81 MHz (9.4 T) on a Bruker MSL 400P spectrometer. The ^{29}Si NMR spectra were measured with 40° pulses, spinning rates of 5.0–5.5 kHz, and 35 s recycle delays. Chemical shifts are quoted in ppm from TMS. The single-quantum (“normal”) ^{23}Na NMR spectra were measured using short and powerful radio frequency pulses (0.6 μs , equivalent to 15° pulse angle), a spinning rate of 15 kHz, and a recycle delay of 2 s. Chemical

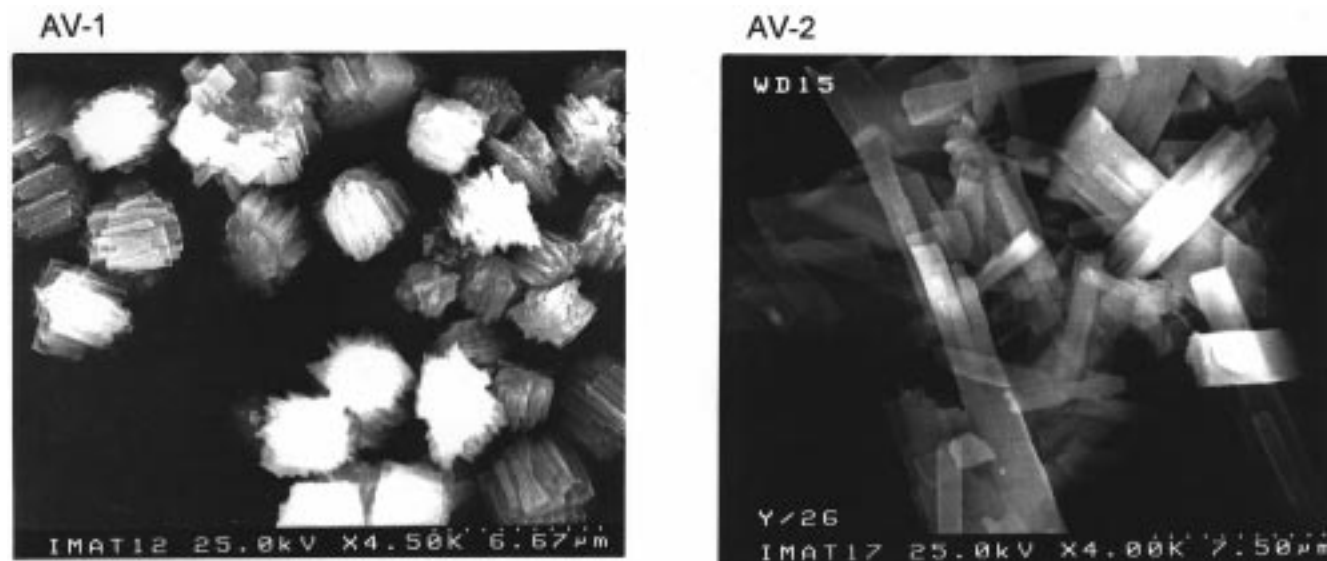


Figure 1. SEM images of AV materials. AV-1 and AV-2 are the synthetic analogues of minerals montregianite and rhodesite, respectively.

shifts are quoted in ppm from 1 M (aqueous) NaCl. $3Q$ ^{23}Na MAS NMR spectra were recorded with radio frequency magnetic field amplitudes of ca. 125 kHz; 256–450 data points were acquired in the t_1 dimension in increments of 8–9 μs . To produce pure absorption line shapes in the $3Q$ MAS spectra, the optimum conditions for excitation and transfer of the ($\pm 3Q$) coherences using a simple two-pulse sequence were used.¹⁴ The phase cycling was composed of 24 phases for the selection of $3Q$ coherences. This phase cycling was combined with a classic overall four-phase cycle in order to minimize phase and amplitude mis-settings of the receiver. The ppm scale was referenced to ν_0 frequency in the ν_2 domain and to $3\nu_0$ in the ν_1 domain (reference 1 M aqueous NaCl). Thermogravimetric curves were measured on a TGA-50 Shimadzu analyzer. The samples were heated under air with a rate of 5 $^\circ\text{C}/\text{min}$. Bulk chemical analysis data were collected for all AV materials studied. These were also routinely characterized by Raman and diffuse-reflectance ultraviolet spectroscopies and differential scanning calorimetry, but these data will not be presented here.

Results and Discussion

Scanning Electron Microscopy and Powder X-ray Diffraction. Figure 1 shows SEM micrographs of AV materials. The powder XRD patterns of AV-1 and montregianite⁹ are shown in Figure 2. The small differences observed are mainly due to the fact that extensive framework substitution of Y and Si by Ca, Mg, Ba, and Al, respectively, occurs in the mineral.⁹ The unit cell parameters of AV-1 have been calculated assuming a monoclinic unit cell ($P2_1/n$, $Z = 2$)¹⁰ and cell dimensions $a = 9.595$ Å, $b = 23.956$ Å, $c = 9.583$ Å, $\beta = 93.850^\circ$. Moreover, the powder XRD reveals (baseline in the range 22–35 $^\circ$ 2θ slightly raised) that AV-1 contains a small amount of amorphous impurity. The crystal structure of AV-1 and montregianite consists of two different types of layers alternating along the $[010]$ direction (Figure 3a): (a) a double silicate sheet, where the single silicate sheet (Figure 3c) is of the apophyllite type with four- and eight-membered rings, and (b) an open octahedral sheet composed of $[\text{YO}_6]$ and three distinct $[\text{NaO}_4(\text{H}_2\text{O})_2]$ octahedra (Figure 3d).¹⁰ The layers are parallel to the (010) plane. The K atoms are 10-coordinate, and the six water molecules are located within large channels formed by the planar eight-membered silicate rings.

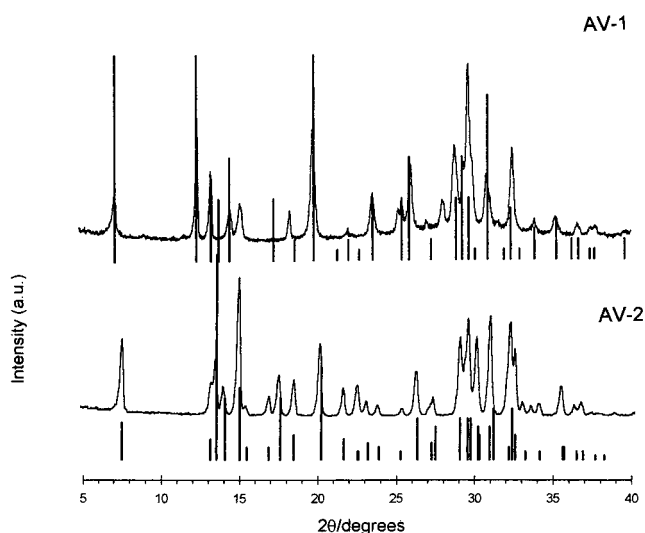


Figure 2. Powder XRD patterns of AV materials. For comparison, the solid lines depict the montregianite and rhodesite reflections, respectively.

The powder XRD patterns of AV-2 and rhodesite¹⁰ (Figure 2) are shown in Figure 2. AV-2 is orthorhombic with $a = 23.797$ Å, $b = 7.031$ Å, $c = 6.598$ Å. The crystal structure of AV-2 and rhodesite consists of silicate double layers, chains of edge-sharing $[\text{Ca}(\text{O}, \text{OH})_2]_6$ octahedra, and potassium cations and additional water molecules within the pores of the silicate double layers (Figure 3b,c,e).¹³ Rhodesite and montregianite have double silicate layers of the same topology. In fact, other minerals such as delhayelite, hydrodelhayelite, and macdonaldite, all have similar double silicate sheets.¹³ In rhodesite these layers possess the maximum topological symmetry ($P2mm$), while in montregianite all symmetry has been lost. The structure of rhodesite contains two sets of octahedrally coordinated calcium ions which form single chains parallel to $[001]$ (Figure 3e). The octahedral chains connect adjacent silicate double layers. While Ca(2) is coordinated to six terminal oxygens that belong to six different $[\text{SiO}_4]$ tetrahedra, Ca(1) is coordinated to four terminal oxygens from four $[\text{SiO}_4]$ and two oxygens which are part of water molecules. The extraframework potassium ions are 10-coordinated to six bridging oxygens and four water molecules.

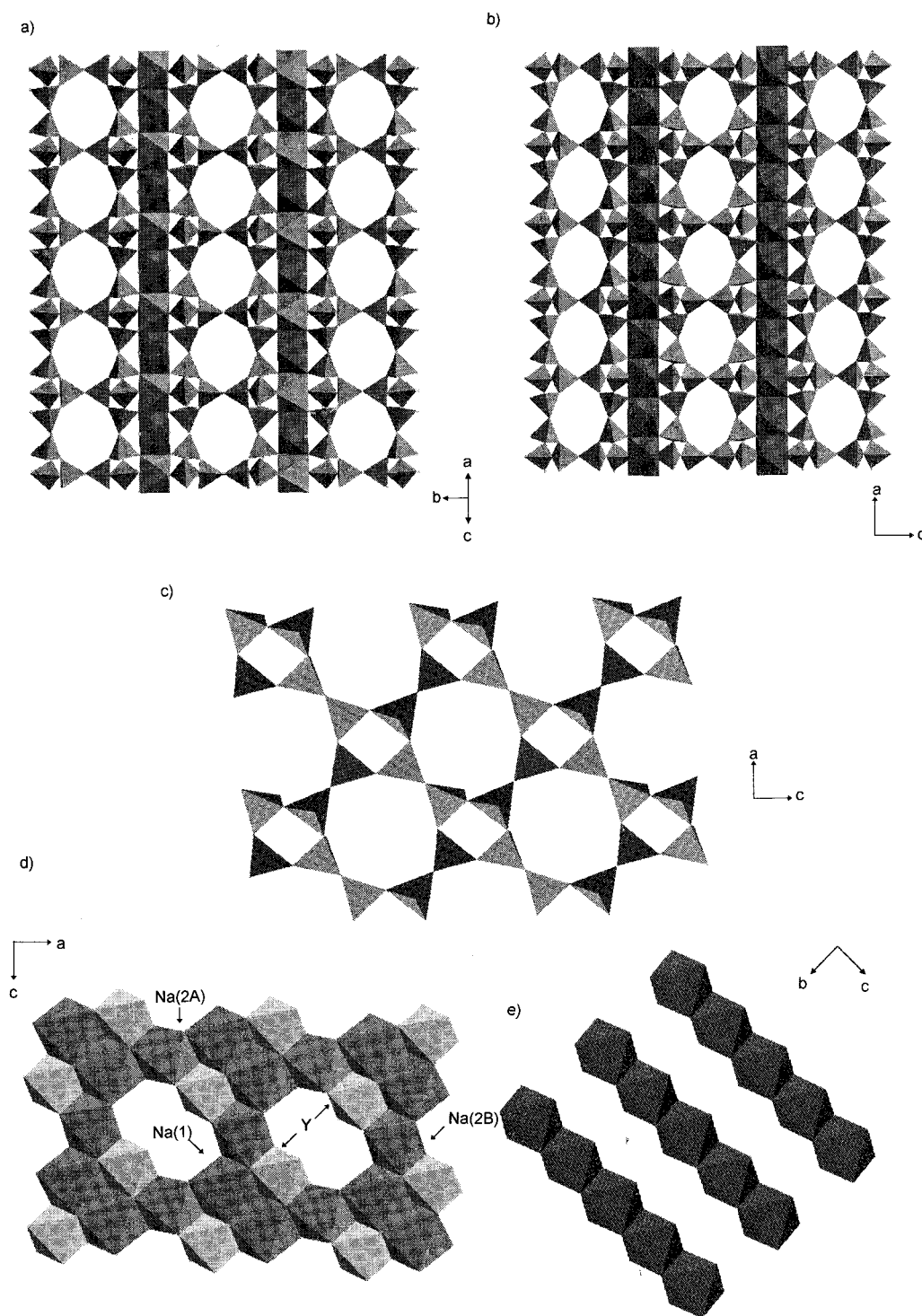


Figure 3. Schematic views of the structures of (a) montregianite (AV-1) and (b) rhodesite (AV-2). Note the alternating octahedral sheet and double silicate layer. (c) Apophyllite-type single silicate sheet. (d) Montregianite open octahedral sheet consisting of Y and three different Na octahedra; rhodesite chains of Ca edge-sharing octahedra.

It is instructive to compare the octahedral layers of montregianite and rhodesite.¹³ In both solids there are two sets of octahedra, which are occupied by Ca^{2+} in rhodesite and by Y^{3+} and Na^+ in montregianite. Calcium ions have the right size (ionic radius 1.00 Å) to form straight chains of edge-shared octahedra in rhodesite (Figure 3e). In montregianite, the slightly smaller (0.90 Å) yttrium ions can, in combination with sodium ions [Na(2A) and Na(2B)], still adjust to the drier chains of double layers. The voids between these octahedral chains are occupied by sodium ions [Na(1)], leading to the formation of a

layer of face-sharing polyhedra (Figure 3d). Since only 50% of the interchain positions are filled by Na(1), these layers are perforated.

²⁹Si and ²³Na MAS NMR. The ²⁹Si MAS NMR spectrum of AV-1 (Figure 4) displays two groups of resonances in the ranges -96 to -102 ppm and -105 to -108 ppm. The spectrum can be deconvoluted into eight peaks with equal intensities, revealing the presence in AV-1 of eight nonequivalent Si sites. In accord with this observation, the crystal structure of montregianite calls for the presence of eight unique Si sites

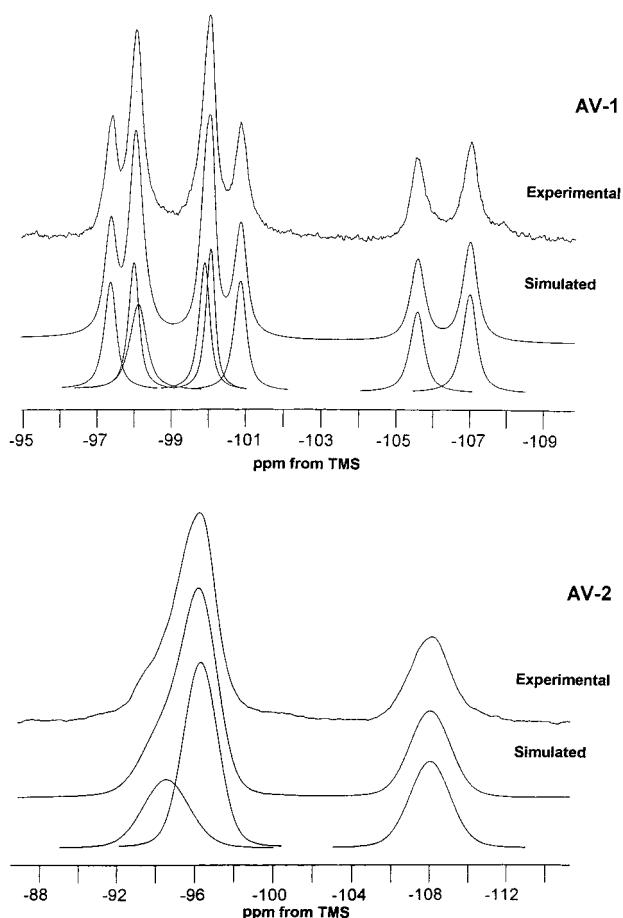


Figure 4. ^{29}Si MAS NMR spectra of AV-1 and AV-2.

with equal populations.¹⁰ Two silicate tetrahedra [Si(1) and Si(4)], one each within the four-membered rings belonging to a single sheet, have upward-pointing apexes [O(1)], which are shared with the apexes of the two downward-pointing corresponding tetrahedra [Si(4) and Si(1), respectively] in the second silicate sheet.¹⁰ Clearly, Si(1) and Si(4) are Si(4Si) environments (Si linked to four other Si via oxygen bridges) and the ^{29}Si MAS NMR resonances at -105.5 and -106.9 ppm are attributed to them. The assignment of the peaks at high frequency is more difficult. Si(6) is of the type Si(3Si, 1Y). Si(6)–O(12) is the shortest nonbridging bond length (1.562 Å) involving the most charge-deficient oxygen, which is bonded to a Y atom.¹⁰ Considering the well-known correlation between the ^{29}Si chemical shifts and the SiO bond lengths in silicates,¹⁵ we tentatively assign the peak at -100.8 ppm to Si(6). The other five unique Si atoms are connected to three other silicons via bridging oxygens.¹⁰ However, the fourth oxygen atom is nonbridging and is bonded to one Y and two Na atoms. [Si(2a) and Si(2b)] and [Si(5a) and Si(5b)] have very similar local environments, and thus the resonances overlapping at ca. -98 and ca. -100 ppm are probably associated with these sites. The resonance at -97.3 ppm is assigned to the remaining Si(3) site.

The ^{29}Si MAS NMR spectrum of AV-2 (Figure 4) displays two peaks, at -96 (with a high-frequency shoulder) and -108.0 ppm. The spectrum can be deconvoluted into three resonances centered at -94.5 , -96.3 , and -108.0 ppm with relative intensities 1:2:1 (spinning sidebands included), revealing the presence in AV-2 of three nonequivalent Si sites. In accord with this observation, the crystal structure of montregianite calls for the presence of three unique Si sites with 1:2:1 populations.¹³ In rhodesite each silicon atom is tetrahedrally coordinated by

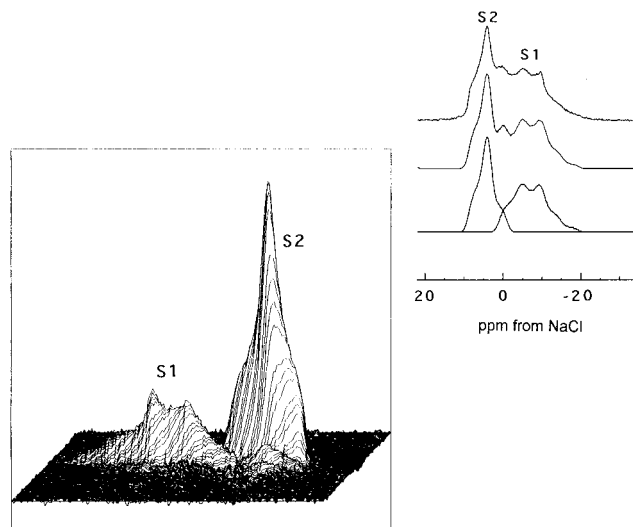


Figure 5. ^{23}Na 3Q MAS NMR spectrum of AV-1. The inset depicts the "normal", experimental, and simulated, single-quantum spectrum.

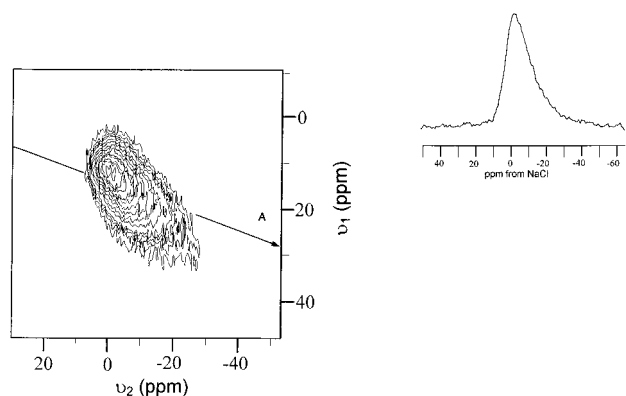


Figure 6. ^{23}Na 3Q MAS NMR spectrum of AV-2. The inset depicts the "normal", single-quantum spectrum.

four oxygens. Three [Si(1) and Si(3)] out of four [SiO_4] tetrahedra share three corners with adjacent [SiO_4] tetrahedra and one corner with a $[\text{Ca}(\text{O}, \text{OH})_2]_6$ octahedron. The fourth [Si(2)] shares all four corners with adjacent [SiO_4] tetrahedra. The peak at -108.10 ppm is, thus, attributed to Si(2). Since the populations of sites Si(1) and Si(3) are in a 2:1 ratio, the former gives the resonance at -96.3 ppm, while the latter gives the peak at -94.5 ppm.

The ^{23}Na triple-quantum (3Q) MAS NMR spectrum¹⁶ of AV-1 (Figure 5) displays two resonances with intensities close to 1:1. Although montregianite contains three nonequivalent Na sites, the $[\text{Na}(2\text{A})\text{O}_4(\text{H}_2\text{O})_2]$ and $[\text{Na}(2\text{B})\text{O}_4(\text{H}_2\text{O})_2]$ octahedra (populations 0.47 and 0.45, respectively) are very similar in configuration, and it is unlikely that they can be distinguished by solid-state ^{23}Na NMR.¹⁰ The $[\text{Na}(1)\text{O}_4(\text{H}_2\text{O})_2]$ site (population 0.95) forms a weak seventh bond with O(5B) and is, thus, distorted. The 3Q peak S1 displays a relatively broad powder pattern and, hence, is ascribed to the distorted Na(1) site. S2 is assigned to sites Na(2A) and Na(2B). The single-quantum ("normal") spectrum (see inset in Figure 5) can be simulated assuming the presence of two resonances, ascribed to sites Na(1) and [Na(2A) and Na(2B)], with intensities of ca. 1:0.9 and the following parameters: isotropic chemical shifts 1.8 and 9.0 ppm; quadrupole coupling constants 1.92 and 1.24 MHz; asymmetry parameters 0.50 and 1.0, respectively.

The ^{23}Na 3Q MAS NMR spectrum of AV-2 (Figure 6) contains a single, broad, peak, which is not aligned with the

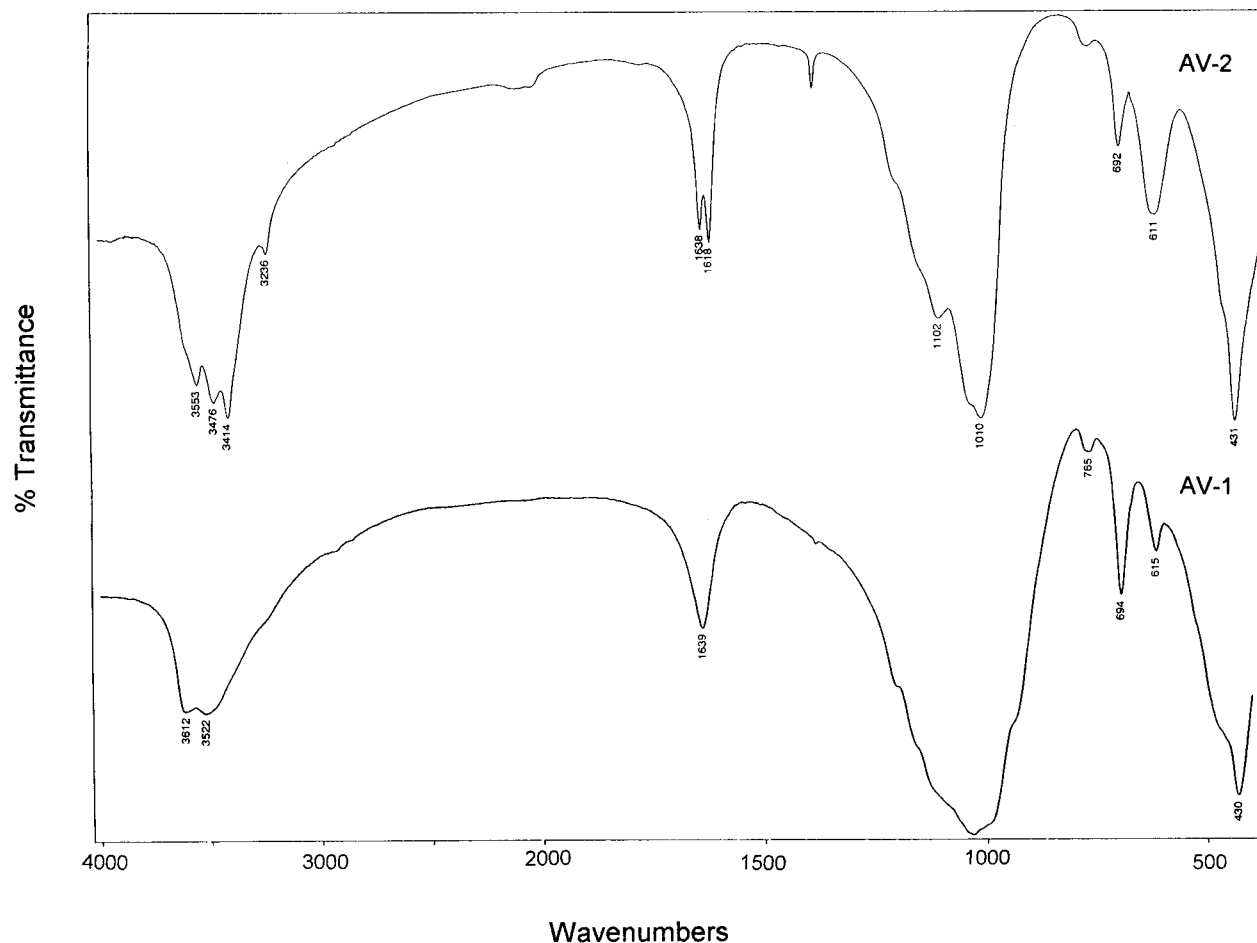


Figure 7. FTIR spectra of AV-1 and AV-2.

so-called anisotropic axis A,¹⁴ revealing a relatively large distribution of both quadrupole constants and chemical shifts. Clearly, in AV-2 the sodium ions are distributed. To rationalize this observation, we now briefly discuss the sodium distribution in rhodesite. There has been some debate as to whether rhodesite contains sodium ions in its structure. Hesse et al. studied this subject in detail and arrived at the following conclusions.¹³ In their structure refinements the four octahedral chain-linking sites per unit cell (denoted C sites) were (a) all occupied (such as in mineral delhayelite), (b) all empty (rhodesite, macdonaldite, and hydrodelhayelite), or (c) two of these sites were fully occupied, the other two unoccupied (montregianite). This suggests that partial site occupation is possible for those C sites that are empty in ideal stoichiometric crystals. Such is the case of rhodesite. In the presence of high sodium concentrations the rhodesite C sites may be partially occupied by Na⁺. In fact, ideal stoichiometric rhodesite seems to be the sodium-free end member, HKCa₂Si₈O₁₉·6H₂O, of the solid solutions HK_{1-x}Na_{x+2y}[Si₈O₁₉]·(6-z)H₂O. Our synthetic analogues of rhodesite, which were prepared in the presence of sodium, probably do not correspond to stoichiometric rhodesite; rather they correspond to intermediate members of the solid solution. Hence, in AV-2 the local sodium environments are slightly different, and it is not unexpected that the ²³Na 3Q MAS NMR spectra reveal a distribution of spectral parameters.

Fourier Transform Infrared Spectroscopy. The FTIR spectrum of AV-1 (Figure 7) and the mineral montregianite⁹ are very similar. Here, we follow closely the spectral assignments given in ref 10 for montregianite. In particular, the medium-intensity band at 1639 cm⁻¹, due to the H-O-H

bending, confirms that water is present in the structure. Three O-H stretching bands are observed in the range 3400–3700 cm⁻¹. The band at 3612 cm⁻¹ is assigned to water molecules W(4), W(5), and W(6), which are bonded to one nonframework K atom each. The band at 3522 cm⁻¹ is given by the water molecule W(3), which is bonded to K and is probably hydrogen-bonded to W(4) and W(5). The shoulder at 3460 cm⁻¹ is assigned to water molecules W(1) and W(2), which are part of the octahedral layer. Both water molecules are bonded to two Na atoms, and in addition, one H atom in each one may be H-bonded to two oxygen atoms. The FTIR spectrum of AV-2 is shown in Figure 7. As in montregianite and AV-1, the bands at 1618 and 1638 cm⁻¹ indicate the presence of zeolitic water. Three O-H stretching bands are, again, observed in the range 3400–3700 cm⁻¹. The detailed assignments of the bands at 3553, 3476, and 3414 cm⁻¹ are not entirely clear, although it is likely that they follow the attributions discussed for montregianite.

Thermal Stability. Thermogravimetry data (not shown) provide further evidence that the structures of AV-1 and montregianite⁹ are very similar. The dehydration of AV-1 is essentially complete at ca. 450–500 °C, and the total mass loss is 11.4%. AV-1 materials calcined at 650 °C and rehydrated in air, overnight at room temperature, display TGA curves similar to the parent solid. Three stages of dehydration occur, at 20–80 °C [loss of disordered zeolitic water molecules adsorbed within the channels], 80–220 °C [loss of water W(4), W(5), and W(6)], and 200–450 °C [loss of water W(1) and W(2)].¹⁰ The dehydration of AV-2 is terminated at about 500 °C, and the total mass loss is 11.2%. Three stages of

dehydration occur, at 20–160 °C, 240–310 °C, and 310–430 °C. The solid can be rehydrated reversibly in air, overnight at room temperature, when it is calcined at temperatures up to 500 °C.

Acknowledgment. We would like to thank FEDER and PRAXIS XXI for financial support.

References and Notes

- (1) Szostak, R. *Molecular Sieves*; Van Nostrand Reinhold: New York, 1989.
- (2) Kuznicki, S. M. US Pat., 485.320.2, 1989.
- (3) Anderson, M. W.; Terasaki, O.; Ohsuna, T.; Philippou, A.; Mackay, S. P.; Ferreira, A.; Rocha, J.; Lidin, S. *Nature* **1994**, 367, 347.
- (4) Anderson, M. W.; Terasaki, O.; Ohsuna, T.; O'Malley, P. J.; Philippou, A.; MacKay, S. P.; Ferreira, A.; Rocha, J.; Lidin, S. *Philos. Mag. B* **1995**, 71, 813.
- (5) Anderson, M. W.; Philippou, A.; Lin, Z.; Ferreira, A.; Rocha, J. *Angew. Chem., Int. Ed. Engl.* **1995**, 34, 1003.
- (6) Rocha, J.; Brandão, P.; Lin, Z.; Ferreira, A.; Anderson, M. W. *J. Phys. Chem.* **1996**, 100, 14978.
- (7) Lin, Z.; Rocha, J.; Brandão, P.; Ferreira, A.; Esculcas, A. P.; Pedrosa de Jesus, J. D.; Philippou, A.; Anderson, M. W. *J. Phys. Chem.* **1997**, 101, 7114.
- (8) Rocha, J.; Ferreira, P.; Lin, Z.; Brandão, P.; Ferreira, A.; Pedrosa de Jesus, J. D. *Chem. Commun.* **1997**, 2103.
- (9) Chao, G. Y. *Can. Mineral.* **1978**, 16, 561.
- (10) Ghose, S.; Gupta, P. K. S.; Campana, C. F. *Am. Mineral.* **1987**, 72, 365.
- (11) Mountain, E. D. *Mineral. Magn.* **1957**, 31, 607.
- (12) Hesse, K.-F. Z. *Kristallogr.* **1987**, 178, 98.
- (13) Hesse, K.-F.; Liebau, F. Z. *Kristallogr.* **1992**, 199, 25.
- (14) Rocha, J.; Esculcas, A. P.; Fernandez, C.; Amoureux, J. P. J. *Phys. Chem.* **1996**, 100, 17889.
- (15) Engelhardt, G.; Michel, D. *High-Resolution Solid-State NMR of Silicates and Zeolites*; Wiley: New York, 1987.
- (16) Medek, A.; Harwood: J. S.; Frydman, L. *J. Am. Chem. Soc.* **1995**, 117, 12779.